



September 7. - 9.9.2009

Cheb, Czech Republic

# STUDY OF INTEGRAL ARRANGEMENT OF MHD PUMPS TRANSPORTING MOLTEN METALS OR SALTS

DR. VÁCLAV KOTLAN  
PROF. IVO DOLEŽEL  
ASSOC. PROF. BOHUŠ ULRYCH

**Abstract:** *The paper deals with one of the fundamental possibilities of improving magnetohydrodynamic (MHD) pumps based on the integration of effects of elementary MHD minipumps distributed along the pipe through which they transport the considered liquid. The crucial point of the work consists in computer modeling of this integral arrangement (system of minipumps) and presentation of the results that demonstrate their advantages—reduction of electric currents flowing through the minipumps and consequent reduction of the total ohmic losses in the system.*

**Key words:** *Electric field, magnetic field, hydraulic loop, hydraulic losses, ohmic losses, finite element method.*

## INTRODUCTION

High-temperature nuclear reactors and also modern operator-free minireactors use for transfer of thermal energy from the active zone molten metals (Na, Pb, Pb-Bi) or molten salts (such as fluoride salts). Pumping of these liquid media by classical mechanical radial or axial pumps is, however, rather difficult and the lifetime of such devices is relatively low.

More prospective are, therefore, electromagnetic pumps without movable parts. The simplest devices of this kind are magnetohydrodynamic (MHD) pumps with magnetic field generated either by a system of appropriately arranged saddle coils carrying direct current or by a system of permanent magnets.

These problems were discussed in details in [1]–[3] and mainly in [4], where, however, just one pump was taken into account; the presented paper represents its natural continuation and extends its ideas. It was shown, that despite several advantages the solution with one pump may have even one serious drawback. Since the magnetic flux density of existing magnetic circuits built from permanent magnets is limited by about 2T, the relevant pump requires from time to time (mainly in case of molten salts or during transients – for example at the startup of the reactor) relatively high electric currents (or current densities) passing through the working medium (see Fig. 1 and par. 2).

This problem is solved by using the integration of effects of MHD minipumps distributed uniformly along a certain part of the pipe. The crucial point of the work consists in computer modeling of this integral pump and presentation of the results that demonstrate their advantages—reduction of electric currents flowing through the minipumps and consequent reduction of the total ohmic losses in the system.

## 1 FORMULATION OF THE PROBLEM

### 1.1 The principle of operation of MHD pumps

The principle of the MHD effect for pumping electrically conductive nonferromagnetic liquids (nonferromagnetic molten metals, molten salts or also ionic liquids) follows from Fig. 1. Perpendicularly to the channel with the working medium **1** there flows direct current  $I_e$  between two nonferromagnetic (and in case of molten metals and salts also heatproof) electrodes **E1** and **E2**. The vector of its density  $\mathbf{J}_e(x, y, z)$  is prevalingly oriented in parallel with axis  $x$ , thus perpendicularly to the axis  $z$  of the channel. In case that magnetic field is generated by a system of permanent magnets, then these magnets must produce a field whose density  $\mathbf{B}_m(x, y, z)$  is prevalingly oriented in parallel to axis  $y$ , thus practically perpendicularly to the axis  $z$  of the channel and to the

vector  $\mathbf{J}_e(x, y, z)$ . The mutual interaction of these two vectors gives rise to the Lorentz force  $\mathbf{F}_L$  in the working medium, whose vector is parallel to axis  $z$  and pushes this medium upwards.

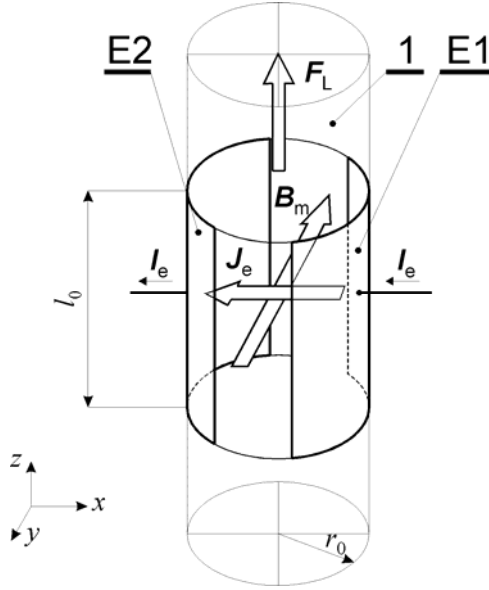


Fig. 1: Principal scheme of MHD pump  
1 – channel with working medium, E1, E2 – electrodes

The following Fig. 2 shows the distribution of electrodes for the

- classical conception of the MHD pump (two electrodes, see Fig. 2a),
- integral conception of the MHD pump ( $2N_e$  electrodes, see Fig. 2b).

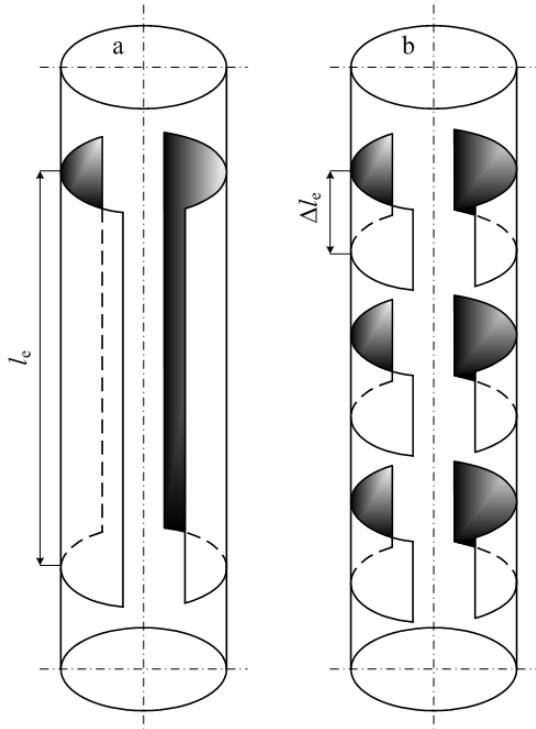


Fig. 2: Arrangement of the electrodes of MHD pump  
a – two electrodes of length  $l_e$   
b –  $2N_e$  electrodes of length  $\Delta l_e = l_e / N_e$

In order to obtain sufficient information about the operation of the pump in both classical and “integral” arrangements we have chosen a loop in which the transfer of coolant can be realized by both types of pumps, independently of one another.

## 1.2 Basic parameters of the considered cooling loop

Investigated is a cooling loop of a miniature high-temperature nuclear reactor RAPID (10 MWT, 1 MWE) proposed by the Central Research Institute of Electric Power Industry (CRIEPI), Japan [5]. Details concerning the loop from the viewpoint of the MHD pump can be found in [4] or [6]. The basic constructional and physical parameters of this loop and also physical parameters of the cooling medium together with the requirements on the MHD pump are summarized in Tab. 1.

Tab. 1. basic information about the cooling loop

Parameter	Symbol	Dimension	Value
diameter of the pipe (and pump)	$D_0 = 2r_0$	[m]	0.075
Working medium: fluoride salt (*)			
operation temperature	$T_{\text{work}}$	[°C]	690
specific mass	$\rho$	[kg/m <sup>3</sup> ]	1972
electrical conductivity	$\gamma_{\text{el}}$	[S/m]	501.3
thermal conductivity	$\lambda_T$	[W/(m°C)]	0.9194
specific heat	$c_p$	[J/(kg °C)]	1850
kinematic viscosity	$\nu$	[m <sup>2</sup> /s]	$1.255 \times 10^{-6}$
Further thermal and hydraulic parameters			
thermal output of the reactor	$P_{\text{th}}$	[MW]	10
maximal. temperature of coolant	$T_{\text{max}}$	[°C]	775
minimal temperature of coolant	$T_{\text{min}}$	[°C]	625
mass flow rate of coolant	$G_c$	[kg/s]	36.04
volume flow rate of coolant	$V_c$	[m <sup>3</sup> /s]	0.01828
flow rate in the pipe of cooling loop	$w$	[m/s]	1
hydrodynamic pressure in the cooling loop(**)	$\Delta p_{\text{hd}}$	[Pa]	714
hydrodynamic force in the cooling loop	$F_{\text{hd}}$	[N]	3.154
total Lorentz force in the cooling loop(***)	$F_L$	[N]	4.731 $\approx 5$
<b>MHD pump (classical arrangement)</b>			
internal diameter	$D_0$	[m]	0.075
length	$l_e$	[m]	0.3

magnetic field	$B_{a,y}$	[T]	1.533
electric current	$I$	[A]	52.83
ohmic losses	$P_e$	[W]	11.63

(\*) composition LiF-NaF-KF (45.3-13.2-41.5 [mol %])  
(\*\*) for details see [6], Tab. 3  
(\*\*\*) generated by an MHD pump with safety coefficient  $\kappa_b = 1.5$

The constructional arrangement of the cooling loop for minireactors RAPID is depicted in Fig. 3.

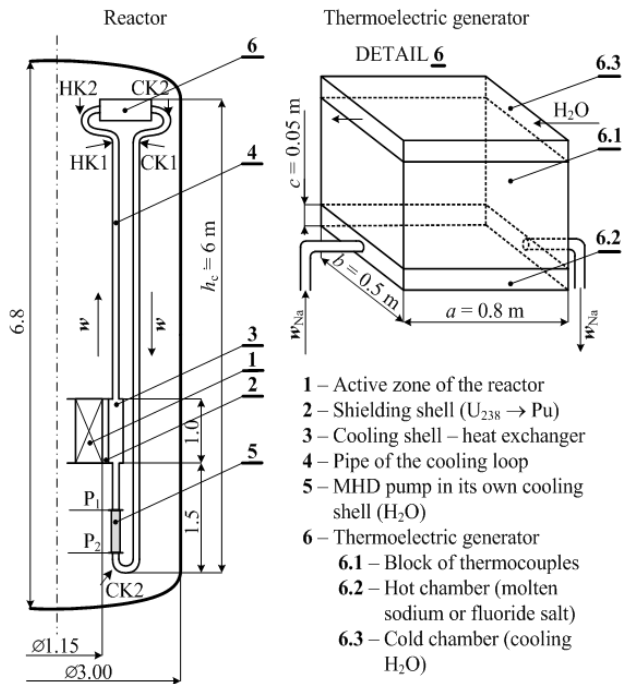


Fig. 3. Arrangement of the considered cooling loop for minireactors RAPID

## 2 MATHEMATICAL MODELS OF THE CONSIDERED PUMPS

### 2.1. Preparatory computations

In the process of designing any pump (even the MHD pumps) it is first necessary to determine the requirements on its operation, i.e.,

- arrangement of the working loop (open, closed),
- physical parameters of the transported liquid,
- mass and volume flow rate and corresponding velocity of flow,
- hydrostatic pumping lead (if it exists),
- hydrodynamic losses in the working loop that have to be overcome by the pump.

A general algorithm for the relevant computations can be found in references [7]–[9].

A detailed algorithm of the considered cooling loop according to Fig. 3 is described in [6], par. 3.2 and 5.2, the corresponding input data and results are summarized in the same paper in Tab. 1. The solution was carried out on the assumptions that

- the loop is closed and fully filled with the cooling medium (no hydrostatic forces have to be overcome),
- considered is the steady-state working regime, with-

out inertial forces acting in the medium.

On these conditions the force acting on the medium is constant and its value  $F_L = 4.731 \approx 5$  N. For this force we have to design the MHD pump, see par. 2.2.

For the sake of simplicity we consider here an MHD pump in the classical arrangement, with two electrodes of length  $l_e$ . In the case of the “integral” arrangement of the pump all presented relations are quite similar, but their formal appearance is rather complicated.

### 2.2. Mathematical models

First, it is necessary to calculate the distribution of magnetic field (produced by the system of permanent magnets, see [10] and Fig. 4) and electric field generated by the system of electrodes (see Fig. 5). The next step is to determine the current density in the working medium between the electrodes (for the calculated magnetic field) that secures the required Lorentz force  $F_L$ .

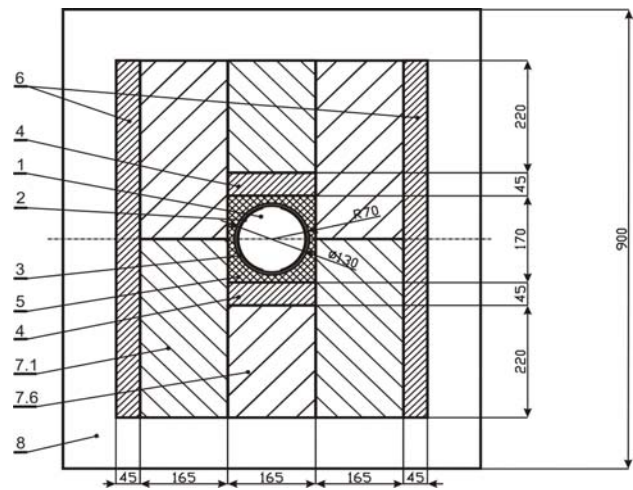


Fig. 4. Cross-section of an MHD pump with magnetic field generated by a system of permanent magnets 1-transported liquid metal or salt, 2-electrodes (austenitic steel CSN 17 241), 3- pipe (molten basalt), 4-ferromagnetic focusators, 5-thermal insulation of magnets (glass wool), 6-ferromagnetic bypasses of magnetic flux (carbon steel CSN 12 040), 7.1–7.6-permanent magnets (NdFeB Magnet, Grade GSN-40, [10]), 8-cooling water

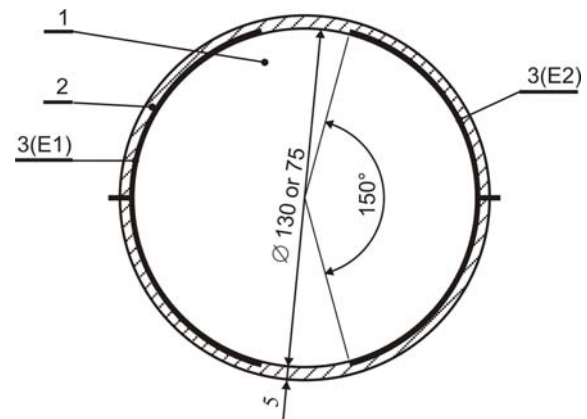


Fig. 5. Electric circuit of the considered MHD I-transported liquid metal or salt, 2-pipe (molten basalt), 3-electrodes,

It is, moreover, necessary to check the steady-state temperature field in the system in order to verify whether the working temperature of the permanent magnets is lower than the maximal permissible value (otherwise the parameters of the magnets strongly deteriorate).

### 2.2.1. Electric, magnetic and temperature fields in the MHD pump

Provided that all three fields are stationary, independent of time, we can describe them (see [11], [12]) by a system of three independent partial differential equations describing

- **electric field**

$$\Delta\varphi = 0 \quad (1)$$

and

$$\mathbf{J}_e = -\gamma_{el} \cdot \text{grad}\varphi. \quad (2)$$

- **magnetic field** produced by a system of permanent magnets of coercive force  $\mathbf{H}_c$  and remanence  $\mathbf{B}_r$

$$\text{curl}\left(\frac{1}{\mu} \text{curl} \mathbf{A} - \mathbf{H}_c\right) = \mathbf{0} \quad (3)$$

where

$$\mu = \frac{B_r}{H_c} = \text{const}$$

and

$$\mathbf{B}_m = \text{curl} \mathbf{A}. \quad (4)$$

- **temperature field**

$$\text{div}(\lambda \text{grad} T) = -\mathbf{J}_e^2 / \gamma_{el} \quad (5)$$

The vector of electromagnetic force  $\mathbf{F}_L$  acting on electrically conductive working medium (molten metal or salt) in the working channel of volume  $V$  is given by the relation

$$\mathbf{F}_L = \int_V (\mathbf{J}_e \times \mathbf{B}_m) dV \quad (6)$$

The physical parameters of particular elements of the MHD pumps occurring in the above equations are given in Tab. 2.

Equations (1), (3) and (5) may be solved by some of professional codes (see par. 3).

### 2.2.2. Determination of current density $\mathbf{J}_e$ and current $I_e$ securing the required electromagnetic force $\mathbf{F}_L$ .

Equation (6) for the considered channel of circular cross-section yields

$$J_{a,x} = \frac{F_L}{B_{a,y} \frac{\pi D_0^2}{4} l_e}, \quad (7)$$

where  $J_{a,x}$  is the average value of the  $x$ -component of vector  $\mathbf{J}_e$  in the cross-section of the working channel,  $F_L$  is the module of the required electromagnetic force,  $B_{a,y}$  is the average value of the  $y$ -component of magnetic flux density in the channel,  $D_0$  is the internal radius

of the channel and  $l_e$  denotes its length.

Tab. 2: Basic physical parameters of materials used in the considered MHD pumps

Item (*)	Element of the pump	Material	Characteristic quantities
1	transported cooling medium	molten fluoride salts	see Tab. 1
2	electrodes	austenitic steel ČSN 17 030	$\gamma_{el} = 1.5 \times 10^6$ [S/m]
			$\mu_r = 1$ [-]
3	shell of the channel	molten basalt	$\gamma_{el} = 1 \times 10^{-6}$ [S/m]
			$\mu_r = 1$ [-]
			$\lambda = 2$ [W/(mK)]
4	ferromagnetic focusators	carbon steel ČSN 12 040	$\mu_r$ see Fig. 6
			$\lambda$ see Fig. 7
5	thermal insulation of magnets	glass wool	$\gamma_{el} = 1 \times 10^{-6}$ [S/m]
			$\mu_r = 1$ [-]
			$\lambda = 0.04$ [W/(mK)]
6	ferromagnetic bypasses	carbon steel ČSN 12 040	$\mu_r$ see Fig. 6
			$\lambda$ see Fig. 7
7	permanent magnets	NdFeB Magnet, Grade GSN-40, [10]	$H_c = 9.555 \times 10^5$ [A/m]
			$B_r = 1.27$ [T]
			$T_w = 150$ [°C]
			$\mu_r = 1.0577$ [-]
8	cooling water	H <sub>2</sub> O	$\mu_r = 1$ [-]
			$T_0 = 20$ [°C]
(*) see Fig. 4			

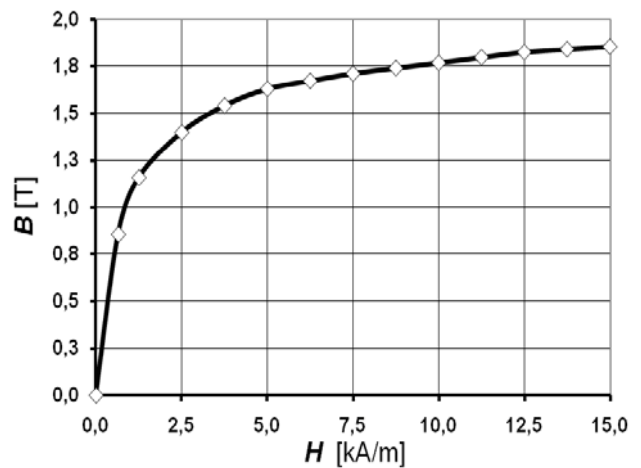


Fig. 6. Magnetization characteristic of carbon steel 12 040 (taken over from [13])

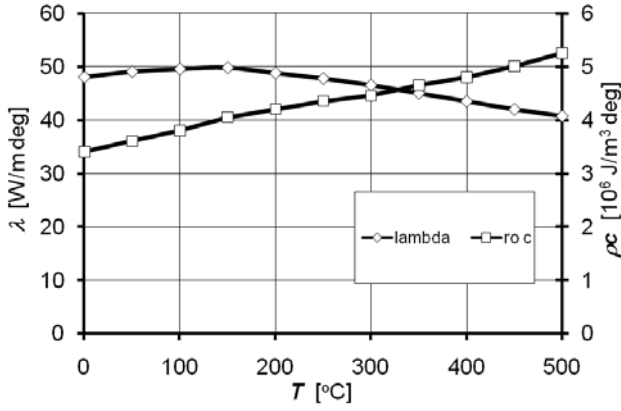


Fig. 7. The temperature dependencies of thermal conductivity  $\lambda$  and heat capacity  $\rho c$  for carbon steel 12 040

At this moment we can (using (7)) determine the value of the required current

$$I_e = J_{a,x} D_0 l_e \quad (8)$$

that must pass between the electrodes **E1** and **E2** (see Fig. 5) in order to produce the force  $F_L$ .

Another important aspect is represented by the indirect boundary conditions for equation (1). Here, it is necessary to find such voltage between the electrodes **E1** and **E2** that secures in the working channel (domain **1** in Fig. 5) the average value of the  $x$ -component of electric field strength

$$E_{a,x} = \frac{J_{a,x}}{\gamma_{el}} \quad (9)$$

This voltage may easily be found, for example, by the “regula falsi” method, see [14].

### 3 COMPUTER MODEL OF THE CONSIDERED MHD PUMPS

The computer model of the considered MHD pumps was realized using the FEM-based program *QuickField* (version 5.6 [15]). The aim was to quickly get information about the approximate, but sufficiently accurate distributions of magnetic, electric and temperature fields – for particulars see par. 4. Great attention was paid to monitoring of the convergence of solution – for results valid in three significant digits it was necessary to use meshes with approximately

- $150 \times 10^3$  nodes for magnetic field,
- $60 \times 10^3$  nodes for electric field,
- $120 \times 10^3$  nodes for temperature field.

Some illustrative results follow. Fig. 8a shows a map of force lines of magnetic field in the system, while Fig. 8b depicts the distribution of equipotentials and vectors  $J_e$  of electric field in the channel. Fig. 8c depicts the steady-state temperature field produced by the transported working medium (see Tab. 1). All results shown in the above figures are valid for sufficiently long MHD pumps, ignoring the front effects.

It is clear that 2D results provide sufficiently accurate qualitative information about the suitability of various considered configurations – for example the total Lorentz force  $F_L$  grows with the homogeneity of the electric and

magnetic fields. Fig. 8c shows, moreover, that the proposal of the thermal insulation **5** (see Fig. 4) is correct; the temperature of permanent magnets **7.1–7.6** does not exceed about  $100^\circ\text{C}$ , which is deep below (see Tab. 2) their maximal operation temperature  $T_w = 150^\circ\text{C}$ . A more detailed presentation and discussion of the results obtained is in par. 4.

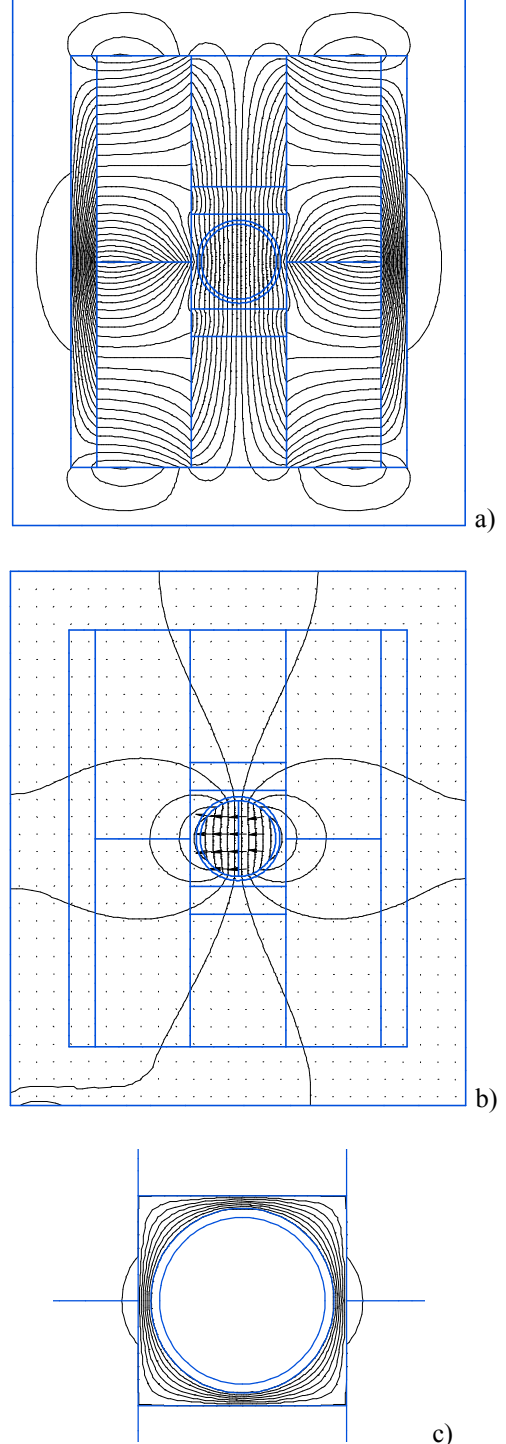


Fig. 8. Illustrative figures of 2D fields in the considered MHD pump (classical arrangement, fluoride salt) calculated by code *QuickField* [15]

- a) magnetic field  
b) electric field  
c) temperature field  $T_{\max} = T_{w,\text{salt}} = 690^\circ\text{C}$ ,  
 $T_{\min} = T_{\text{H}_2\text{O}} = 20^\circ\text{C}$ ,  $\Delta T \approx 80^\circ\text{C}$

## 4 ILLUSTRATIVE RESULTS AND THEIR DISCUSSION

The computations were aimed at answering two basic questions:

### 4.1. Comparison of the MHD in the classical and integral conceptions

This comparison is performed in Tab. 3. From this table we can see that

- if we compare the classical arrangement of length of the working channel  $l_e = 0.3$  m with the integral arrangement of the same length  $l_e = N_e \Delta l_e = 0.3$  m, the current  $I_e$  passing through one pair of electrodes is smaller (the electrodes are “shorter”), but the total ohmic losses  $\Delta P_J$  are the same,
- if we compare the classical arrangement of length of the working channel  $l_e = 0.3$  m with the “integral” pump of greater length (i.e.,  $l_e = N_e \Delta l_e = 1$  m, it is more advantageous from the viewpoints of both the total current  $I_e$  and losses  $\Delta P_J$ ,
- if we compare two “integral” pumps with different numbers of pairs of electrodes, the pump with higher value  $N_e$  of electrodes is more advantageous again.

Tab. 3: Comparison of the classical and “integral” conception of the MHD pump from the viewpoint of current  $I_e$  and total ohmic losses  $\Delta P_J$

		Arrangement of the MHD pump		
		classical	"integral"	
current $I_e$ passing through one pair of electrodes	[A]	$l_e = 0.3$	$l_e = 0.1$ [m]	
		[m]	$N_e = 1$	$N_e = 3$
ohmic losses $\Delta P_J$ due to $N_e$ pairs of electrodes	W	11.63	11.63	3.487

### 4.2. Basic properties of the MHD pumps in the “integral” conception

In this paragraph we examine

- the value of the partial and total ohmic losses  $P_e$  and  $P_{\text{celk}}$ ,
  - the partial and total Lorentz forces  $F_{L,e}$  and  $F_{L,\text{celk}}$ ,
- where the partial quantities are valid for one pair of the electrodes (their total number being  $N_e$ ).

The ohmic losses (compare Figs. 9a and 9b) both between one pair of electrodes  $P_e$  and their total value  $P_{\text{celk}}$  decrease with the number of pairs of electrodes  $N_e$ . This is connected with the analogous decrease of

current  $I_e$  passing through one pair of electrodes. Of course, the total losses  $P_{\text{celk}}$  in the whole pump are greater. Decrease of the height of the electrodes  $\Delta l_e$  also leads to an increase of  $P_e$  and  $P_{\text{celk}}$  due to growth of the resistance of the working medium between the individual pairs of electrodes.

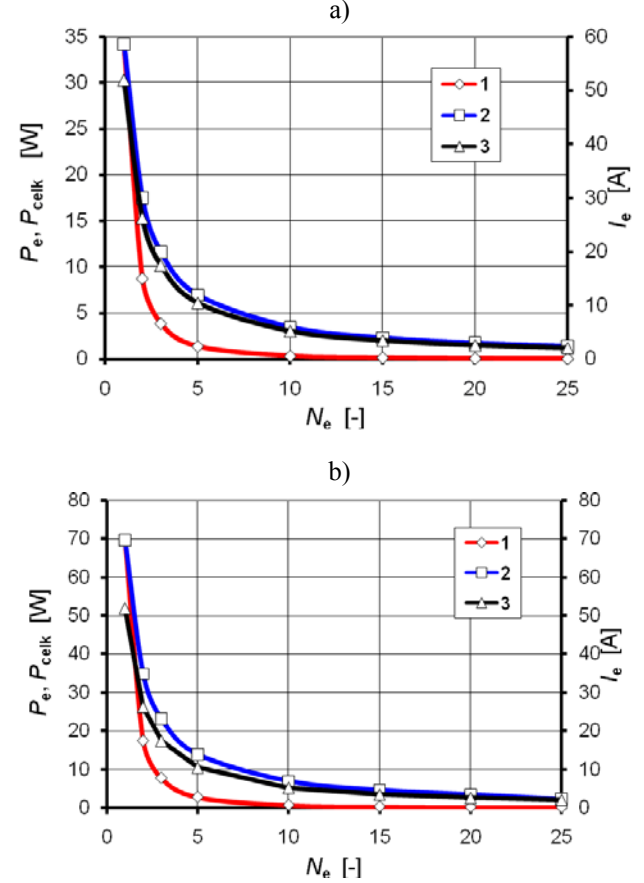


Fig. 9. Partial and total ohmic losses as a function of the number  $N_e$  of the pairs of electrodes for the “integral” MHD pumps

a) up -  $\Delta l_e = 0.1$  m b) down -  $\Delta l_e = 0.3$  m  
1-  $P_e$  [W], 2-  $P_{\text{celk}}$  [W], 3-  $I_e$  [A]

The Lorentz forces  $F_{L,e}$  (Figs. 10a, 10 b) produced by one pair of electrodes decrease with their growing number  $N_e$ . On the other hand, the total force  $F_{L,\text{celk}}$  remains constant and must be equal to the required value high enough to overcome the hydrodynamic losses (see par. 3.1 and 3.2). These forces do not depend on the height of the electrodes  $\Delta l_e$ . This is associated with the fact that with smaller  $\Delta l_e$  we must increase current density in the channel in order to reach the same value of  $F_{L,e}$ .

## 5 CONCLUSION

It could be concluded that from the viewpoint of the physical properties the MHD pump in the “integral” arrangement is more advantageous than the classical MHD pump. The system works with smaller field currents  $I_e$ ,

which results in smaller ohmic losses  $P_{\text{celk}}$ . Another viewpoint, constructional, should be, however, also considered. From this viewpoint the pump is much more complicated. Therefore, it is necessary to evaluate for every particular case all advantages and drawbacks of both conceptions and then make the optimal decision.

The complete description of the considered “integral” pump and its evaluation from all above viewpoints can be found on the www pages <http://147.228.94.30/> of the Czech electronic journal Electroscope.

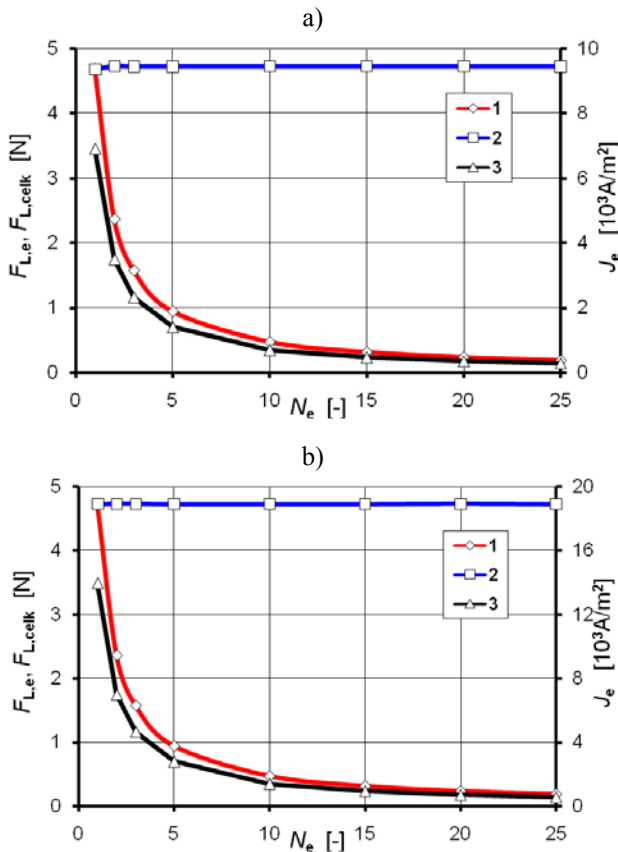


Fig. 10. Partial and total Lorentz forces as a function of the number  $N_e$  of the pairs of electrodes for the “integral” MHD pumps

a) up -  $\Delta l_e = 0.1 \text{ m}$  b) down -  $\Delta l_e = 0.05 \text{ m}$

1-  $F_{L,e}$  [N], 2-  $F_{L,celk}$  [N], 3-  $J_e$  [ $\text{A/m}^2$ ]

## REFERENCES

- [1] Büllow, J., Doležel, I., Karban, P., Ulrych B.: Numerical Analysis of an MHD Minipump with Permanent Magnets Transporting Molten Metal. Vesnik of the Technical University of Lvov, Ukraine, Vol. 43, No. 596, pp. 39–45.
- [2] Doležel, I., Donátová, M., Karban, P., Ulrych, B.: Pumps of Molten Metal Based on Magnetohydrodynamic Principle for Cooling High-Temperature Nuclear Reactors. Przegląd Elektrotechniczny (Electrical Review), 2009, No 4, pp. 13–16.
- [3] Büllow, J., Doležel, I., Karban, P., Ulrych, B.: Numerical Modeling of MHD Effect for Pumping of Molten Metals. Proc. AMTEE 2007, CD-ROM.

- [4] Doležel, I., Kotlan, V., Ulrych, B., Valenta, V.: Magnetohydrodynamic Pumps with Permanent Magnets for Pumping Molten Metals or Salts. Proc. CPEE, Waplewo, Poland, September 2009, accepted.
- [5] Status of Small Reactor Designs without On-Site Refueling. IAEA (International Atomic Energy Agency), Vienna, Aus, 2007, Annex. XVII, Reactor RAPID, pp. 469–489.
- [6] www pages <http://147.228.94.30/>, the Czech electronic journal Electroscope.
- [7] Cengel, Y.A., Turner, R.H.: Fundamentals of Thermal-Fluid Sciences. Mc Graw Hill, NY (USA), 2000.
- [8] Gerbeau, J B., Le Bris, C., Lelievre, T.: Mathematical Methods for the Magnetohydrodynamics of Liquid Metals. OXFORD University Press, Oxford, GB, 2006.
- [9] Idelchik I.E.: Handbook of Hydraulic Resistance. Begell House, Inc (USA), 1996.
- [10] [www.goudsmitmagnets.com](http://www.goudsmitmagnets.com).
- [11] Stratton, J.A.: Electromagnetic Theory. McGraw Hill Book Co., NY 1941.
- [12] Holman, J. P.: Heat Transfer. McGraw Hill Book Co., NY 2002.
- [13] Company Standard ŠKODA 00 6004.
- [14] Ralston, A.: A First Course in Numerical Analysis. McGraw Hill Book Co., NY 1973.
- [15] [www.quickfield.com](http://www.quickfield.com).

**Authors:** Dr. Václav Kotlan, University of West Bohemia, Univerzitni 26, 306 14 Plzen, CR, E-mail: [vkotlan@kte.zcu.cz](mailto:vkotlan@kte.zcu.cz); Prof. Ivo Doležel, Czech Technical University, Faculty of Electrical Engineering, Technická 2, 166 27 Praha, CR, E-mail: [dolezel@fel.cvut.cz](mailto:dolezel@fel.cvut.cz); Assoc. Prof. Bohus Ulrych, University of West Bohemia, Univerzitni 26, 306 14 Plzen, CR, E-mail: [ulrych@kte.zcu.cz](mailto:ulrych@kte.zcu.cz).